Solvent Penetration into Ordered Thin Films of Diblock Copolymers

H. Lin and A. Steyerl

Department of Physics, University of Rhode Island, Kingston, Rhode Island 02881

S. K. Satija and A. Karim

National Institute of Standards and Technology, Gaithersburg, Maryland 20877

T. P. Russell*

IBM Research Division, Almaden Research Center, 650 Harry Road,
San Jose, California 95120-6099

Received September 12, 1994; Revised Manuscript Received November 29, 1994®

ABSTRACT: The penetration of vapors of pure and mixed solvent into ordered thin films of symmetric, diblock copolymers of polystyrene (PS) and poly(methyl methacrylate) (PMMA) was investigated by neutron reflectivity. In the case of cyclohexane, a marginal solvent for PS but a poor solvent for PMMA, only the PS layer at the surface was swollen by the cyclohexane. The underlying multilayered structure was unperturbed by the solvent vapors, which indicates that the first PMMA layer near the surface, *even though it has a thickness of only* ~150 Å, acts as an effective diffusion barrier preventing penetration of the solvent. In the case of a mixed solvent, in particular a 75/25 methanol/toluene mixture, where toluene is a good solvent for both components, the entire multilayer is swollen. However, the swelling of the layers is not uniform as a function of depth. In addition, the appearance of second-order Bragg reflections shows that the swelling of the PS and PMMA layers is not equal.

Introduction

There has been some effort to understand the solvation of diblock copolymers at a solid interface. For example, experiments have been performed on polystyrene–poly(2-vinylpyridine) (PS–PVP) diblock copolymers adsorbed onto quartz from toluene[1] and polystyrene–poly(ethylene oxide) (PS–PEO) diblock copolymers adsorbed onto silicon from toluene.[2] In these cases, the copolymer is dissolved in the solvent and the solution is placed in contact with the solid boundary. In the present study, interest is focused on the interaction of solvent with a diblock copolymer that has ordered on the surface. In particular, to what extent can small molecules penetrate into an ordered system where the molecules interact favorably with either or both of the blocks of the copolymers? Early studies by Ionescu and Skoulios[3] addressed this problem on bulk diblock copolymers where it was found, depending upon the solvent, that swelling of the copolymer could occur volumetrically or only normal to the lamellar period. In these studies, the presence of the substrate and the perfection of the ordering of the lamellar microdomains with respect to the surface play a key role in the swelling behavior.

The surface-induced ordering of symmetric diblock copolymers has been studied extensively.[4–9] In the case of symmetric diblock copolymers of polystyrene (PS) and poly(methyl methacrylate) (PMMA), denoted P(S-*b*-MMA), the copolymer of interest here, alternating layers of PS and PMMA oriented parallel to the surface of the substrate are found. PS is located preferentially at the air–copolymer interface and, in the case of an SiO_2 substrate, PMMA is located at the substrate. The thickness adjacent to the boundaries of the layers is one-half that of the layers inside the film. The period of the multilayer is dictated by the total molecular weight of the copolymer and the interactions between the segments of each block. The thickness of the film at any point is given as $(n + 1/2)L$ for the case mentioned, where n is an integer and L is the period. If the initial film thickness is incommensurate with this restriction, then islands or holes form on the surface with a step height equal to L. The type of surface topography and the fraction of the surface occupied by islands or holes depend upon the initial thickness. However, the multilayering is maintained within the topographical features and at least a half-layer of PS is always located at the surface. Details of the morphology of the islands and holes, in particular the edges of these features, have been discussed recently by Carvalho and Thomas.[10]

The alternating structure of the multilayer presents a unique field for a diffusing species. It would be expected that a solvent that dissolves both blocks would easily penetrate into the multilayered structure. However, unlike the case of a bulk sample, the presence of the solid substrate may present some limitations to the solvent penetration. In the case where the solvent is selective for only one block, the other block will retard the diffusion of the solvent. In addition, defects in the multilayers will provide channels through which the solvent can easily migrate. On one extreme, the diffusion of a homopolymer, corresponding to one of the blocks, *into the multilayered structure* has been studied.[11] There it was found that the homopolymer did not diffuse into the multilayer or at least the diffusion was severely impeded.

In this study, ordered multilayers of P(S-*b*-MMA) in the presence of low molecular weight solvent vapors were investigated by neutron reflectivity. Selective deuteration of either block or the solvent molecules provides an easy means of monitoring the penetration of the solvent into the multilayer. The results of the study show that, in the case of a toluene/methanol mixture, both the PS and PMMA layers are swollen. However, the extent of swelling was found to depend

---

® Abstract published in *Advance ACS Abstracts,* January 15, 1995.

0024-9297/95/2228-1470$09.00/0

upon the distance from the free surface. In the case of cyclohexane, a solvent for PS but a very poor solvent for PMMA, only the PS layer at the free surface was found to be swollen. There was no penetration of the solvent into the underlying multilayered structure. Consequently, even though the PMMA layer adjacent to the surface is only ~150 Å, it is still a very effective barrier to diffusion.

Experiment

Thin films of P(d-S-*b*-MMA) and P(d-S-*b*-d-MMA) were spin coated onto polished, 10 cm diameter, silicon substrates (5 mm thick) from solutions in toluene. The lower case d indicates a perdeuteration of that block. The films were annealed under vacuum at 170 °C for a sufficient time to produce a multilayered structure. P(d-S-b-MMA) has an $M_w = 1.2 \times 10^5$ with $M_w/M_n = 1.12$, whereas P(d-S-*b*-d-MMA) has an $M_w = 1.15 \times 10^5$ with $M_w/M_n = 1.10$. Each copolymer, purchased from Polymer Laboratories, was Soxhlet extracted in cyclohexane to remove PS homopolymer impurity generated during the synthesis.

Swelling studies were performed on the ordered copolymer films by placing the samples in a closed cell in a solvent-saturated environment. The films were exposed to the solvent atmosphere for at least 4 h prior to measurements. Since the reflectivity profiles did not change with time, it was assumed that the solvent was in equilibrium with the vapor. In one set of experiments, cyclohexane was used, which is a solvent for the PS block but a nonsolvent for the PMMA block. In a second set of experiments, a 75/25 methanol/toluene mixture was used. This mixture is a Θ solvent for PS homopolymer at 34 °C, whereas it is a Θ solvent for PMMA homopolymer at 26 °C.[12] All reflectivity measurements were performed at room temperature.

In the case of cyclohexane, the sample was mounted vertically above a reservoir of the solvent at the base of the closed cell. Reflectivity measurements were performed on the BT-7 reflectometer in the reactor hall of the National Institute of Standards and Technology (NIST). A graphite monochromator selected neutrons having a wavelength, λ, of 2.35 Å with $\Delta\lambda/\lambda = 0.02$. In the horizontal direction, the beam had an angular divergence of 0.02°. In the case of the methanol/toluene mixture, reflectivity studies were performed on the NG-7 reflectometer located in the neutron guide hall in the Cold Neutron Research Facility at NIST. Here the samples are mounted horizontally with a solvent reservoir at the base. Neutrons of wavelength 4.1 Å with $\Delta\lambda/\lambda = 0.055$ were used.

In both geometries the specular neutron reflectivity was measured over a neutron momentum transfer, Q, range from 0.005 to 0.15 Å^{-1}. Here, $Q = (4\pi/\lambda) \sin \theta$, where θ is the incidence angle. The specimens were aligned to intercept the neutron beam fully at an incidence angle just below the critical angle which corresponded to a $Q \simeq 0.01$ Å^{-1}. Background was measured with the detector offset from the specular position by ±0.6°. Reflectivity profiles were obtained by subtracting the background from the specular reflectivity data and normalizing to the incident intensity. Data analysis was performed using a recursion method, first introduced by Parratt,[13] with a least squares minimization of the error. This has been discussed in detail elsewhere.[14]

Results and Discussion

Shown in Figure 1a is the neutron reflectivity profile as a function of the momentum transfer, Q, obtained from a P(d-S-*b*-MMA) copolymer on a silicon substrate after annealing at 170 °C for 12 h. As shown in previous studies, the reflectivity profile exhibits distinct interference peaks resulting from a multilayered structure where the d-PS and PMMA lamellar microdomains are oriented parallel to the surface with the more polar PMMA located at the substrate and the lower surface energy PS at the air surface. The thickness of the film was 940 Å before annealing. The equilibrium period, L_0, of this copolymer is 388 Å, with the thickness of the d-PS and PMMA microdomains being 202 and 186 Å, respectively. The scattering length density profile shown in the inset was used to calculate the reflectivity profile shown as the solid line in the figure. The agreement between the calculated and experimental reflectivity profiles is quite good over the entire scattering vector range. The period obtained from this profile agrees quite well with the equilibrium period. In addition, since the initial thickness, t_0, of the film was 940 Å, this corresponds to 2.42 copolymer periods. Therefore, $t_0 \sim (n + 1/2)L_0$ where $n = 2$. Consequently, for this film the surface of the copolymer was flat with no formation of islands or holes on the surface. This was confirmed by independent optical microscopy measurements and is in keeping with the scattering length density profile shown in the inset of Figure 1a. While the data shown here has been presented elsewhere, it does provide a basis for the subsequent swelling measurements.

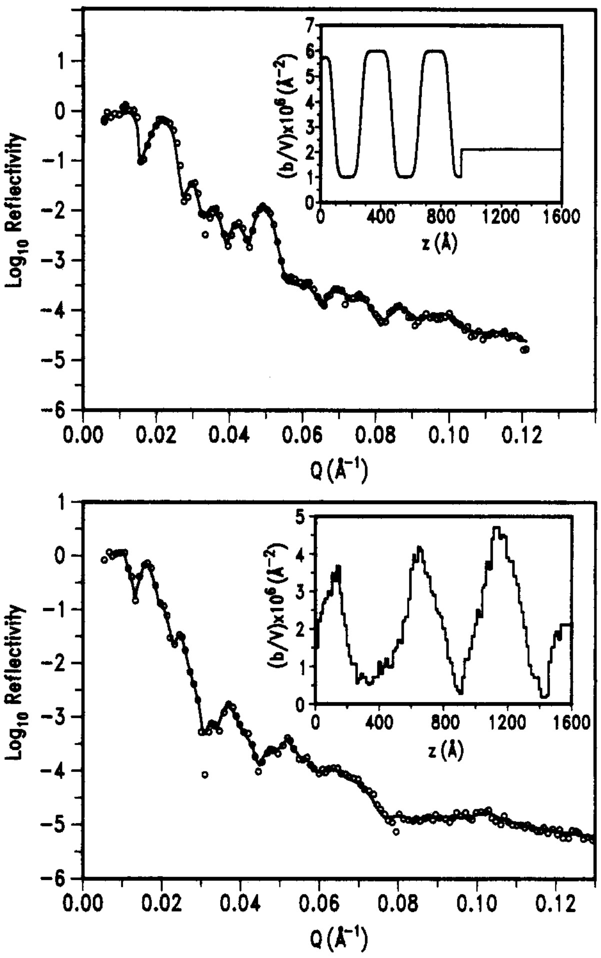

Figure 1. Neutron reflectivity profiles for a P(d-S-*b*-MMA) film of thickness 940 Å in air (a, top) and in the vapor of a 75/25 methanol/toluene mixture (b, bottom). The scattering length density profiles *b/V* are shown in the insets as a function of depth z, where $z = 0$ is the film surface. These profiles yielded the best fits to reflectivity profiles shown as the solid lines in the figures.

If this ordered P(d-S-*b*-MMA) is exposed to vapors of the 25/75 methanol/toluene mixture and allowed to equilibrate, the reflectivity profile shown in Figure 1b is obtained. The swelling of the ordered multilayer has markedly altered the reflectivity results. There is a clear shift in the critical angle to smaller scattering vectors due to the uptake of the protonated solvent which has a lower scattering length density. The swelling has also caused the first-order interference maximum to shift from 0.0212 to 0.0157 Å^{-1}. The period, L, of the copolymer can be determined from

$$\left(\frac{2\pi n}{L}\right)^2 = Q_{\mathrm{obs}}^{\ 2} - Q_{\mathrm{c}}^{\ 2} \qquad (1)$$

where Q_{obs} is the observed peak position, Q_{c} is the critical value of the momentum transfer, and n is an integer corresponding to the order of the reflection. Therefore, the period has increased from 388 Å for the initial copolymer to 529 Å. This represents a 36% increase in the period due to the uptake of the solvent.

A second-order reflection, at $Q = 0.0375$ Å^{-1}, is also evident, indicating that the swelling of the multilayer has not disrupted the lamellar nature of the multilayered structure significantly. Interference fringes, characteristic of the total film thickness, are also evident in the data. From these interference fringes a total film thickness of 1.4×10^3 Å is obtained. In comparison to the initial film thickness of 940 Å, this represents a thickness increase of 49%. Since the total increase in film thickness is not equal to the increase in the period, i.e., 34%, then the swelling of the film by the solvent cannot be uniform. In fact, the swelling at either the air or substrate interface must be greater than that within the film since the interference maxima reflect the internal morphology of the film.

In contrast to the unswollen film, the nonuniformity of the swelling within the film leads to ambiguities in deriving the concentration profile. In fact, it was not possible to use analytic functions to define the concentration. Rather, a histogram approach was used where the width of each step was fixed at 10 Å and the scattering length density of each step in the histogram was allowed to vary. The best fit to the reflectivity profile, indicated by the solid line in the figure, was generated using the scattering length density profiles shown in the inset. It should be noted, however, that mirror images of this profile could equally well describe the experimental data. Due to the ambiguity in the fitting process and the complexity of the scattering length density profile itself, it is difficult to interpret quantitatively the specific details of the concentration profile. However, qualitatively the picture that emerges from the profile is that the periodic structure of the multilayer is maintained and that the contrast between the layers increases as one approaches the substrate. In addition, the overall thicknesses of the swollen layers decrease with increasing depth. Both of these correspond to a situation where the solvent concentration or degree of swelling decreases closer to the substrate.

The width of the interface between the PS and PMMA layers was found to be substantially broadened, making the concentration profile appear as a damped saw tooth. Broadening of the interface would be expected with the introduction of a solvent that would moderate or screen the interactions between the PS and PMMA segments. In the presence of a mutual cosolvent, the effective interaction parameter, χ_{eff}, can be estimated by using mean field arguments for a neutral solvent[15-18] where

$$\chi_{\mathrm{eff}} = \phi_{\mathrm{P}}\chi \qquad (2)$$

Here ϕ_{P} is the volume fraction of polymer and χ is the segmental interaction parameter between PS and PMMA in the bulk. This equation would be expected to be valid for larger ϕ_{P}.[17] ϕ_{P} for the studies here can be estimated as 0.67, the ratio of the as-cast to swollen film thicknesses. This is only approximate and will, of course, vary as a function of depth. The interfacial width, a_{I}, varies as $\chi^{-1/2}$. Therefore

$$(a_{\mathrm{I}})_{\mathrm{S}} = (a_{\mathrm{I}})_0 \phi_{\mathrm{P}}^{\ -1/2} \qquad (3)$$

where $(a_{\mathrm{I}})_{\mathrm{S}}$ is the interfacial width measured in the presence of a solvent for a system having an interfacial width $(a_{\mathrm{I}})_0$ in the bulk. $(a_{\mathrm{I}})_0$ for PS and PMMA is ~40 Å in the absence of capillary waves. Thus, $(a_{\mathrm{I}})_{\mathrm{S}} \simeq 60$ Å. If we assume that the amplitude and wavelengths of the capillary waves are the same in the swollen film, this contributes an additional ~10 Å to the interfacial width measured.[19] Consequently, $(a_{\mathrm{I}})_{\mathrm{S}} \simeq 70$ Å. While this broadening is substantial, the experimental results indicate a greater broadening suggesting that the amplitude of the capillary waves has increased. Given the reduction in the viscosity with the introduction of a common solvent, along with a concomitant decrease in the interfacial tension, relatively broad interfaces would be expected. In addition to this, the restraint of placing a junction point at the interface, representing a large entropic penalty, would be moderated by the introduction of a solvent. Consequently, both entropic and enthalpic arguments can account for substantial broadening.

To remove some of the ambiguity and to examine the effective interfacial widths more closely, the swelling of an ordered film of P(d-S-*b*-d-MMA) was investigated. Shown in Figure 2a is the reflectivity profile of a 1161 Å thick P(d-S-*b*-d-MMA) film annealed at 170 °C for 12 h. The dominant features in the reflectivity profile are the Kiessig fringes arising from the total thickness of the film. The contrast between the d-PS and d-PMMA layers is small since both layers are deuterated and one relies only on the mass density difference between the d-PS and d-PMMA layers. The scattering length density profile shown in the inset was used. Here the characteristic 456 Å period of the copolymer is seen with the total film comprising 2.5 layers. As with the P(d-S-*b*-MMA) case, the surface of the film was flat with no surface topology.

Upon exposing the film to the mixed solvent vapors, the reflectivity profile changes markedly as shown in Figure 2b. Distinct interferences arising from the multilayered structure are evident. The fact that these interferences are so pronounced indicates that the swelling of the d-PS and d-PMMA layers is not equal. If this were the case, then a profile similar to that in Figure 2a would be obtained. The interference maximum at $Q = 0.018$ Å^{-1} corresponds to a multilayer period of 537 Å. In comparison to the period before swelling, this represents an increase in the period of 20%. This is less than the swelling found for the P(S-*b*-d-MMA), which may be due to the higher molecular weight of the P(d-S-*b*-d-MMA) or differences in the interactions of the solvent with the d-PS block.

The scattering length density profile shown in the inset of Figure 2b yielded the best fit to the reflectivity data drawn as the solid line in the figure. As in the case of the P(S-*b*-d-MMA), the swelling is seen to be nonuniform, with the extent of swelling varying as a function of depth. The continuous decrease in the scattering length density of the d-PMMA microdomain and the increase in the scattering length density of the d-PS layer indicate that the swelling of the d-PMMA increases with depth, whereas the d-PS swelling de-

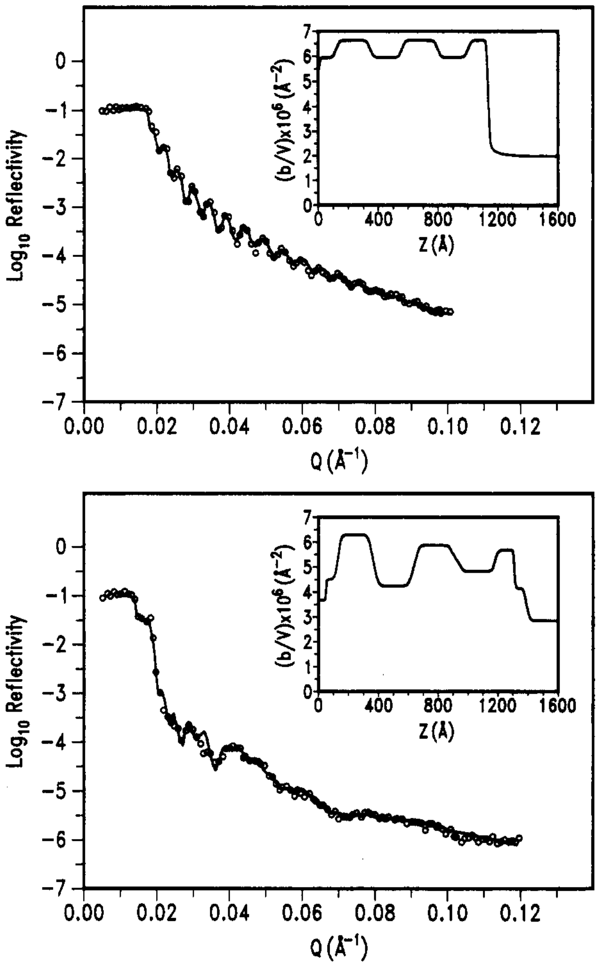

Figure 2. Neutron reflectivity profiles for a P(d-S-*b*-d-MMA) film of 1161 Å thickness in air (a, top) and in the vapor of a 75/25 methanol/toluene mixture (b, bottom). The solid lines are calculated for the scattering length density profiles shown in the insets.

creases with depth. In fact, the swelling of the d-PMMA layer is only $\sim$10% at the air surface and increases to $\sim$17% at the substrate. The d-PS layers, on the other hand, are swollen by $\sim$32% at the air surface and by 24% near the substrate interface. Both the scattering length densities and the thicknesses of the d-PMMA and d-PS layers suggest this. Finally, the width of the interface between the d-PS and d-PMMA layers has increased substantially with swelling from 50 to over 80 Å. This increase of the interfacial width is in keeping with the enthalpic and entropic arguments presented previously.

Consequently, the results on the P(d-S-*b*-d-MMA) and P(S-*b*-d-MMA) indicate that the swelling of copolymer multilayers in a mixed solvent is not uniform. The swelling appears to decrease with increasing depth. At present, however, it is not known if there is a partitioning of the solvent in the multilayers between the PS and PMMA layers. The nonuniformity of the swelling may, in fact, be attributed to the constraint of the copolymer on the substrate laterally. While swelling of the film normal to the surface can occur freely, the film is always limited laterally by the surface area of the substrate. This lateral constraint may, in fact, place limits on the extent of solvent penetration and, consequently, the swelling.

The swelling of the ordered multilayers using cyclohexane is markedly different from that of the methanol/toluene mixture. Cyclohexane is a near-Θ solvent for PS but a nonsolvent for PMMA. The reflectivity profile for a P(d-S-*b*-MMA) multilayer, comprised of 2.5 periods of the copolymer, in cyclohexane vapors is shown in Figure 3. Interferences arising from the multilayered structure are clearly seen in the data. In fact, the overall appearance of these data is quite similar to that in Figure 1a for the initial ordered multilayer. Shown in the inset is the scattering length density profile that yielded the best fit to the reflectivity data. The only difference between this scattering length density profile and that of the initial multilayer is that the scattering length density of the topmost layer of d-PS is diminished.

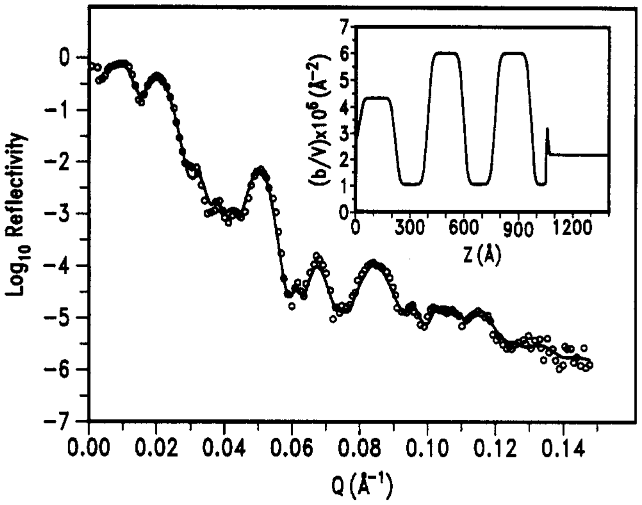

Figure 3. Neutron reflectivity profile for the P(d-S-*b*-MMA) sample in cyclohexane vapor. The solid line was calculated using the scattering length density profile shown in the inset.

Table 1. Scattering Length Densities

	ϱ (g/cm^3)	b/V ($\times 10^6$ Å^{-2})
toluene	0.867	−0.373
methanol	0.791	0.94
75/25 methanol/toluene	–	−0.044
cyclohexane	0.779	−0.278
PS	1.05	1.43
d-PS	1.13	6.1
PMMA	1.15	1.0
d-PMMA	1.24	6.8

From the scattering length densities of d-PS and cyclohexane, given in Table 1, the concentration of cyclohexane in the topmost layer is calculated to be 27%, which corresponds to a swelling of 39%. Outside of this change, the scattering length density is unchanged, demonstrating that the cyclohexane has not penetrated into the multilayer. Stated differently, the 169 Å layer of PMMA acts as a diffusion barrier preventing penetration of the cyclohexane into the interior of the multilayer. One feature that can be inferred from this is that the ordering and orientation of the multilayers are essentially perfect over the entire surface of the film. Any defects would have provided an easy pathway for the solvent to penetrate into the film.

Verification of these results was obtained by swelling an ordered P(d-S-*b*-d-MMA) multilayer with cyclohexane. Since cyclohexane would be expected to swell only the d-PS layers, a marked enhancement in the contrast would be expected. Shown in Figure 4 is the reflectivity profile for P(d-S-*b*-d-MMA) in cyclohexane vapors. Clearly, there are no strong interferences evident in the reflectivity profile, which suggests that the cyclohexane has not penetrated into the film. Shown in the inset is the scattering length density profile that yielded the

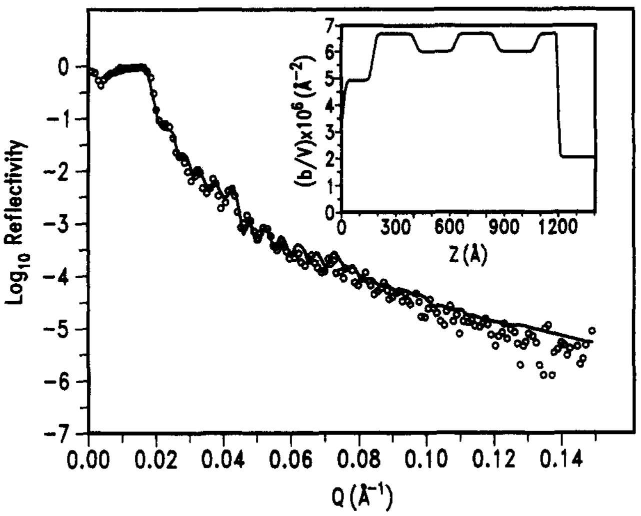

Figure 4. Neutron reflectivity profile for the P(d-S-*b*-d-MMA) sample in cyclohexane vapor. The solid line was calculated using the scattering length density profile shown in the inset.

best fit to the reflectivity data. In keeping with the results from the P(d-S-*b*-MMA), only the scattering length density of the uppermost layer is depressed. From the scattering length density, a cyclohexane concentration of 22% is found, which is in good agreement with the data from the P(d-S-*b*-MMA). Since only the d-PS layer at the surface was swollen by the cyclohexane, one could consider this layer as a grafted brush where the concentration profile would be expected to be of the form[20-22]

$$\phi(Z) = \phi_s\left[1 - \left(\frac{Z}{D}\right)^2\right]^\alpha \qquad (4)$$

Here D is the height of the brush, ϕ_S is the volume fraction of polymer at the grafting surface (which for this case is the interface between the PS and PMMA), and α is the "profile shape" exponent. In a good solvent, $\alpha = 1$, while for the case here (PS in cyclohexane), we expect $\alpha < 0.5$; then the profile will be more steplike. Consequently, the simple step function broadened by a Gaussian, as shown in the inset, was used. The actual shape of the concentration profile, while important, is not the most important finding and should not detract from the observation that such a thin layer of PMMA can act as such an effective diffusion barrier.

The results of these studies should be compared to those of Ionescu and Skoulios on the swelling of bulk, ordered diblock copolymers. In the case of a nonsolvent for one of the blocks, swelling occurs parallel to the lamellar repeat period. In this study effectively no swelling was observed with the exception of the outermost layer. This difference stems from the connectivity of the lamellar microdomains in a bulk sample where stacks of the lamellar microdomains are randomly oriented in the sample. In the case of lamellae oriented parallel to the surface, the perfection of the orientation of the microdomains and the absence of defects in the multilayer preclude the penetration of the solvent. In the case where the solvent will swell or dissolve both blocks, a typical volumetric swelling occurs in bulk samples where a distinct increase in the period occurs. While an increase in the period was found for the copolymers near a surface, the copolymers are confined laterally by the substrate. Consequently, most, if not all, of the swelling occurs in a direction normal to the surface or along the repeat period.

In conclusion, specular reflectivity measurements on the swelling of P(S-*b*-MMA) diblock copolymer multilayers in the vapor of selective and nonselective solvents have been performed. In the case of a good solvent for each block, in particular a 75/25 methanol/toluene mixture, the solvent was found to penetrate into all layers of the multilayer. However, the swelling was not uniform as a function of depth and was not the same for each block. In the case of cyclohexane, a selective solvent for PS, only the d-PS block at the air surface was swollen, with no penetration of the solvent into the underlying multilayer.

Acknowledgment. We are grateful to Mr. J. Micciche, Mr. U-Ser Jeng, and Dr. M. L. Crow (Department of Physics, University of Rhode Island) for building the sample cell used in this project and to Dr. Drexel for help in some of the computational aspects of the work. This work was supported by the U.S. Department of Energy, Division of Materials Science, under Contract DE-FG02-91ER45445 and by the Department of Physics, University of Rhode Island. T.P.R. acknowledges the partial support of the U.S. Department of Energy, Office of Basic Energy Sciences, under Contract FG03-88ER-45375.

References and Notes

(1) Field, J. B.; Toprakcioglu, C.; Dai, L.; Hadziioannou, G.; Smith, G.; Hamilton, W. *J. Phys. II (Fr.)* **1992**, *2*, 2221.
(2) Motschmann, H.; Stamm, M.; Toprakcioglu, C. *Macromolecules* **1991**, *24*, 3681.
(3) Ionescu, M.-L.; Skoulios, A. *Makromol. Chem.* **1976**, *177*, 257.
(4) Anastasiadis, H.; Russell, T. P.; Satija, S. K.; Majkrzak, C. F. *Phys. Rev. Lett.* **1989**, *62*, 8152.
(5) Russell, T. P.; Coulon, G.; Deline, V. R.; Miller, D. C. *Macromolecules* **1989**, *22*, 4600.
(6) Anastasiadis, S. H.; Russell, T. P.; Satija, S. K.; Majkrzak, C. F. *J. Chem. Phys.* **1990**, *92*, 5677.
(7) Foster, M. D.; Sikka, M.; Singh, N.; Bates, F. S.; Satija, S. K.; Majkrzak, C. F. *J. Chem. Phys.* **1992**, *96*, 8605.
(8) Sikka, M.; Singh, N.; Karim, A.; Bates, F. S.; Satija, S. K.; Majkrzak, C. F. *Phys. Rev. Lett.* **1993**, *70*, 307.
(9) deJeu, W. H.; Lambooy, P.; Vahnin, D. *Macromolecules* **1993**, *26*, 4973.
(10) Carvalho, B.; Thomas, E. L. *Phys. Rev. Lett.*, in press.
(11) Green, P. F.; Russell, T. P.; Jérôme, R.; Granville, M. *Macromolecules* **1988**, *21*, 3266.
(12) *Polymer Handbook*, 3rd ed.; Brandup, J.; Immergut, E. H., Eds.; Wiley-Interscience: New York, 1989.
(13) Parratt, L. G. *Phys. Rev.* **1954**, *95*, 359.
(14) Russell, T. P. *Mater. Sci. Rep.* **1990**, *5*, 171.
(15) Hashimoto, T.; Sasaki, K.; Kawai, H. *Macromolecules* **1984**, *17*, 2812.
(16) Sasaki, K.; Hashimoto, T. *Macromolecules* **1984**, *17*, 2818.
(17) Onuki, A.; Hashimoto, T. *Macromolecules* **1989**, *22*, 879.
(18) Helfand, E.; Tagami, Y. J. *J. Chem. Phys.* **1972**, *56*, 3592.
(19) Shull, K. R.; Mayes, A. M.; Russell, T. P. *Macromolecules* **1993**, *26*, 1993.
(20) Satija, S. K.; Majkrzak, C. F.; Russell, T. P.; Sinha, S. K.; Sirota, E. B.; Hughes, G. J. *Macromolecules* **1990**, *23*, 3860.
(21) Milner, S. T. *Science* **1991**, *251*, 905.
(22) Karim, A.; Satija, S. K.; Douglas, J. F.; Ankner, J. F.; Fetters, L. J. *Phys. Rev. Lett.*, submitted.

MA941258A